HHS Public Access

Author manuscript

Free Radic Biol Med. Author manuscript; available in PMC 2024 November 01.

Published in final edited form as:

Free Radic Biol Med. 2023 November 01; 208: 221–228. doi:10.1016/j.freeradbiomed.2023.08.016.

Under peroxisome proliferation acyl-CoA oxidase coordinates with catalase to enhance ethanol metabolism

Xue Chen[a], **Krista L. Denning**[b], **Anna Mazur**[a], **Logan M. Lawrence**[b], **Xiaodong Wang**[c], **Yongke Lu**[a]

[a]Department of Biomedical Sciences, Joan C. Edwards School of Medicine, Marshall University, 1700 3rd Avenue, Huntington WV 25755, USA

[b]Department of Pathology, Joan C. Edwards School of Medicine, Marshall University, 1 John Marshall Drive, WV 25755, United States

[c]Department of Pathology, Guiqian International General Hospital, 1 Dongfeng Ave., Wudang Guiyang, Guizhou 550018, PR China

Abstract

In peroxisomes, acyl-CoA oxidase (ACOX) oxidizes fatty acids and produces H_2O_2, and the latter is decomposed by catalase. If ethanol is present, ethanol will be oxidized by catalase coupling with decomposition of H_2O_2. Peroxisome proliferator-activated receptor α (PPARα) agonist WY-14,643 escalated ethanol clearance, which was not observed in catalase knockout (*Cat*$^{-/-}$) mice or partially blocked by an ACOX1 inhibitor. WY-14,643 induced peroxisome proliferation via peroxin 16 (PEX16). PEX16 liver-specific knockout (*Pex16*$^{Alb\text{-}Cre}$) mice lack intact peroxisomes in liver, but catalase and ACOX1 were upregulated. Due to lacking intact peroxisomes, the upregulated catalase and ACOX1 in the *Pex16*$^{Alb\text{-}Cre}$ mice were mislocated in cytosol and microsomes, and the escalated ethanol clearance was not observed in the *Pex16*$^{Alb\text{-}Cre}$ mice, implicating that the intact functional peroxisomes are essential for ACOX1/catalase to metabolize ethanol. Alcohol-associated liver disease (ALD) is a spectrum of liver disorders ranging from alcoholic steatosis to steatohepatitis. WY-14,643 ameliorated alcoholic steatosis but tended to enhance alcoholic steatohepatitis. In mice lacking nuclear factor erythroid 2-related factor 2 (*Nrf2*$^{-/-}$), WY-14,643 still induced PEX16, ACOX1 and catalase to escalate ethanol clearance and blunt alcoholic steatosis, which was not observed in the PPARα-absent *Nrf2*$^{-/-}$ mice (*Pparα*$^{-/-}$/*Nrf2*$^{-/-}$) mice, suggesting that WY-14,643 escalates ethanol clearance through PPARα but not through Nrf2.

Graphical Abstract

Corresponding information: Yongke Lu, luy@marshall.edu.

Conflict of Interest: None

Declaration of interests

The authors declare that they have no known competing financial interests or personal relationships that could have appeared to influence the work reported in this paper.

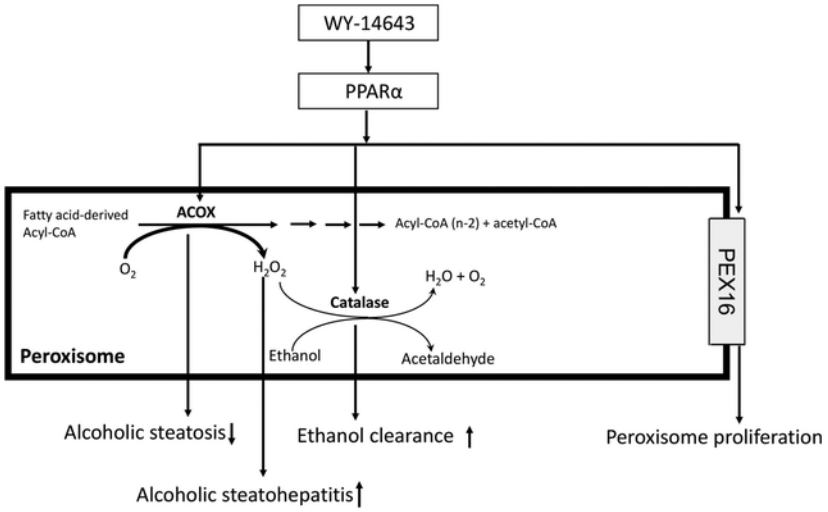

Keywords

WY-14,643; PPARα; Nrf2; PEX16; Alcohol-associated liver disease

INTRODUCTION

Ethanol metabolism is linked to alcohol-associated liver disease (ALD), a spectrum of liver disorders ranging from alcoholic fatty liver (steatosis) to steatohepatitis, fibrosis, cirrhosis, and even liver cancer. Liver is a major organ for ethanol metabolism (1). Ethanol is mainly metabolized to acetaldehyde, and acetaldehyde is further oxidized to acetate by aldehyde dehydrogenase (ALDH), especially by mitochondrial ALDH2. There are 3 major enzymatic systems that metabolize ethanol to acetaldehyde: alcohol dehydrogenases (ADH), microsomal ethanol oxidation system (MEOS), and catalase. In cytosol, ADH metabolizes ethanol to acetaldehyde and reduces NAD^+ to NADH. The increased ratio of NADH/NAD^+ may inhibit fatty acid β-oxidation (FAO) and lead to triglyceride (TG) accumulation in liver, i.e., fatty liver (1). MEOS is mainly derived from smooth endoplasmic reticulum (ER). Chronic ethanol consumption leads to induction of MEOS, and cytochrome P450 2E1 (CYP2E1) is a major alcohol-inducible enzyme in MEOS (2). CYP2E1 metabolizes ethanol by oxidizing NADPH and produces reactive oxygen species (ROS). CYP2E1-mediated oxidative stress contributes to the development of ALD (2–4).

Catalase is mainly in peroxisomes. Like mitochondria, peroxisomes oxidize fatty acids (5). Usually, very long chain and branch chain fatty acids are oxidized in peroxisomes and the resultant shorter chain fatty acids will be further oxidized in mitochondria. The first reaction of peroxisomal FAO is catalyzed by the rate-limiting enzyme acyl-CoA oxidase (ACOX), which produces hydrogen peroxide (H_2O_2) as a byproduct, and the generated H_2O_2 is locally decomposed by peroxisomal catalase (6). There are two steps for catalase to decompose H_2O_2. First, catalase binds one molecular H_2O_2 to form a catalase-H_2O_2 complex. When the catalase-H_2O_2 complex binds a second H_2O_2, both H_2O_2 will be decomposed by catalase and generate 2 molecules of H_2O and 1 molecule of O_2. If ethanol

is present, the ethanol will replace the second H_2O_2 to bind the catalase-H_2O_2 complex, and the ethanol and H_2O_2 are metabolized to acetaldehyde and H_2O, respectively, but no O_2 is formed (7–9). Catalase metabolism of ethanol is stimulated by free fatty acids (FFA), which is attributed to the increased H_2O_2 generation from the peroxisomal FAO (10,11).

Generally, catalase is deemed to play a minor role in ethanol metabolism. However, recently we and another group separately reported that catalase metabolism of ethanol was enhanced by WY-14,643, a potent peroxisome proliferator-activated receptor α (PPARα) agonist (12–15). It is well known that PPARα regulates peroxisomal FAO (16,17), and PPARα activation by WY-14,643 prevents hepatic TG accumulation in experimental ALD model (18). Thus, in peroxisomes, both lipid metabolism and ethanol metabolism are enhanced by PPARα activation. It is plausible that an interaction between lipid metabolism and ethanol metabolism is present in peroxisomes.

WY-14,643 also induces peroxisome proliferation, which was not observed in PPARα knockout (*Pparα* $^{-/-}$) mice (16). Peroxisomes may arise from pre-existing peroxisomes through division and growth. Peroxisomes are also generated *de novo* by budding from ER. Peroxisomal membrane proteins are synthesized in the ER and peroxisomal matrix proteins are synthesized in cytosols (19). Peroxisomes require a group of proteins called peroxins (PEX) for their assembly and division. PEX16, PEX3, and PEX19 are critical for the assembly of the peroxisomal membrane and import of peroxisomal membrane proteins. PEX16 acts as a docking site on the peroxisomal membrane for recruitment of PEX3. PEX3 functions as a docking receptor for PEX19, and PEX19 is a soluble chaperone to function as an import receptor for newly synthesized peroxisomal membrane proteins (20). Thus, PEX16 plays a pivotal role in the peroxisome biogenesis. The loss of PEX16 results in the complete absence of any peroxisomal structures in patients (21). In this study, we examined the effects of peroxisome proliferation on ethanol metabolism and lipid metabolism in mice.

MATERIALS and METHODS

Animals and Treatment

Colonies of *Pparα*$^{-/-}$ mice (#008154, ref. 22), nuclear factor erythroid 2-related factor 2 (Nrf2) knockout (*Nrf2*$^{-/-}$) mice (#017009, ref. 23), *Pex16* flox mice (*Pex16*$^{fl/fl}$ mice; #034155) and Alb-Cre mice (#003574) were purchased from Jackson Laboratory. Catalase knockout (*Cat*$^{-/-}$) mice were derived from *Cat*$^{+/-}$ mice (cryo recovered from Mutant Mouse Resource & Research Center (MMRRC # 036739-MU, ref. 24). The *Pex16*$^{fl/fl}$ mice were crossed with the Alb-Cre mice to create liver-specific Pex16 knockout (*Pex16*$^{Alb\text{-}Cre}$) mice. The *Pparα*$^{-/-}$ mice were crossed with *Nrf2*$^{-/-}$ mice to create *Pparα*$^{-/-}$/*Nrf2*$^{-/-}$ mice. All the mice were housed in temperature-controlled animal facilities with 12-hour light/dark cycles and were permitted consumption of tap water and Purina standard chow *ad libitum*. The mice received humane care. All *in vivo* experiments were approved by the Institution Committee of Animal Use and Care (IACUC) at Marshall University.

Eight to ten weeks old female mice were selected for the Lieber-DeCarli model. Female mice were selected because they reveal a propensity to more severe ALD (25). The mice were fed the control liquid diet (Bio-Serv, Frenchtown, NJ) for 3 days followed by the

ethanol liquid diet for 18 or 25 days (indicated in legends). The concentrations of ethanol in the liquid diet were gradually increased from 10% calories from ethanol to 35%. The control group was continually fed the control liquid diet. WY-14,643 (Cayman, Ann Harbor, MI) was mixed in the liquid diet at 10 mg/L. After overnight fasting, the mice were sacrificed. Blood was collected for serum biochemical assays. The livers were weighted, and liver index was calculated as liver weight/100g body weight. The liver aliquots from the same lobes of different mice were put in neutral Formalin buffer for preparing paraffin sections for Hematoxylin & Eosin staining (H&E). The other liver tissue aliquots were stored at −80°C.

Male mice have been suggested for acute or acute-on-chronic model because they are more resistant to the mortality than female mice (26). The 8–9 weeks old male mice were fed the Lieber-DeCarli ethanol diet containing 0–20 mg/L WY-14,643 for 2 weeks followed by a gavage of 5 g/kg ethanol. Some WY-14,643-fed mice were treated with ACOX1 specific inhibitor 10,12-tricosadiynoic acid (TrA) (27), which was injected intraperitoneally (10 mg/kg) twice at 24h and 30 min before the ethanol gavage. Seven hours later blood was collected for serum ethanol assay.

Time course of WY-14,643 induction of peroxisome proliferation: C57BL/6J mice were fed the control liquid diets containing WY-14,643 (0–20 mg/L) for 1–5 days. The liver was collected for peroxisomal membrane protein and matrix protein detection by Western blotting analysis.

Ethanol clearance test: The 8–9 weeks old mice were fed the control liquid diets containing WY-14,643 (0–20 mg/L) for 1 day or 2 weeks, followed by a single dose of ethanol at 2.5 g/kg by gavage. The blood was collected for ethanol assay in various time points via retro-optical sinus under anesthesia by isoflurane.

Biochemical assays and Western Blotting analysis: The isolated serum was used for measuring TG, ethanol, FFA, β-hydroxybutyrate and alanine transaminase (ALT). The liver tissues were homogenized in 0.15M KCl to make homogenates. The liver homogenates were subjected to 10,000 rpm (Rotor 75Ti) for 20 min, and the supernatants were further centrifuged at 40,000 rpm for 1 h, the final supernatants are cytosols, and the pellets are microsomes. The homogenates, cytosols and microsomes were used for Western blotting analyses. Rabbit anti-CYP2E1 is a generous gift from Dr. Jerome Lasker (Hackensack Biomedical Research Institute, Hackensack, NJ). Commercially available assay kits and primary antibodies are listed in Supplemental Table 1.

Statistical analysis—Results are expressed as mean ± S.D. Statistical evaluation was carried out by using two-way analysis of variance (ANOVA) with subsequent the Student-Newman-Keuls post hoc test. $P<0.05$ was considered as statistical significance.

RESULTS and DISCUSSION

Peroxisome matrix protein ACOX1 and catalase are upregulated in the *Pex16*$^{Alb\text{-}Cre}$ mice

In the *Pex16*$^{Alb\text{-}Cre}$ mice, peroxisomal membrane protein PEX16 was undetectable, but peroxisome matrix protein ACOX1 and catalase were upregulated in the *Pex16*$^{Alb\text{-}Cre}$

mice (Supplemental-Fig. 1A). The upregulated ACOX1 and catalase were detected in both microsomes (Supplemental-Fig. 1B) and cytosol (Supplemental-Fig. 1C), but in the cytosol ACOX1 and catalase were increased to a greater extent than in microsomes (Supplemental-Fig. 1D) because they are soluble matrix proteins. Hepatomegaly (increased liver index) was also observed in the *Pex16*$^{Alb\text{-}Cre}$ mice (Supplemental-Fig. 1E). PEX16 mutation is one of genetic causes of Zellweger syndrome (21). The patients with Zellweger syndrome also display hepatomegaly (28). In skin fibroblasts isolated from Zellweger syndrome patients, catalase is upregulated and located in cytoplasm (29). Thus, hepatomegaly and the cytosolic upregulation of peroxisome matrix enzymes in the *Pex16*$^{fl/fl}$ mice reflects the human pathological condition.

PEX16 was induced by WY-14,643 in the *Pex16*$^{fl/fl}$ mice (Fig. 1A). PEX16 is an integral membrane protein (30), so it was not detected in cytosol, but GAPDH, a cytosolic protein, was detected in cytosol but not in microsomes (Fig. 1B). Another peroxisome membrane protein PMP70, a marker of peroxisomes, was also induced by WY-14,643, which was observed in the *Pex16*$^{fl/fl}$ mice but not in the *Pex16*$^{Alb\text{-}Cre}$ mice (Fig. 1A). ACOX1 and catalase were also induced by WY-14,643 in the *Pex16*$^{fl/fl}$ mice, but in the *Pex16*$^{Alb\text{-}Cre}$ mice, the already increased ACOX1 and catalase were not further induced by WY-14,643 (Fig. 1A). ACOX1 and catalase are water soluble peroxisome matrix protein, so they were detectable in cytosol (Fig. 1B). WY-14,643-inducible CYP4A, a PPARα-regulated protein located in ER rather than in peroxisomes, was also upregulated in the *Pex16*$^{Alb\text{-}Cre}$ mice but was not further induced by WY-14,643 (Fig. 1B). The upregulated CYP4A in the *Pex16*$^{Alb\text{-}Cre}$ mice was not detectable in cytosol (Fig. 1B).

Peroxisomal matrix proteins are translated in free ribosomes in the cytoplasm with peroxisomal targeting sequences (PTSs) allowing proteins to be shuttled to peroxisomes. PEX5 is the import receptor for PTS1-containing proteins and PEX7 is for PTS2-containing proteins (20). In Zellweger syndrome patients, catalase protein but not mRNA was upregulated, suggesting that a posttranslational but not transcriptional mechanism is involved (29). However, in *C. elegans*, knockdown of *prx-5*, the homolog of human PEX5 coding gene, triggers transcriptional upregulation of *ctl-2*, the homolog of human catalase coding gene, in a manner dependent on NHR-49, the homolog of PPARα (31). In the *Pex16*$^{Alb\text{-}Cre}$ mice, PPARα is probably also responsible for the upregulation catalase and ACOX1 because PPARα-regulated microsomal CYP4A was also upregulated (Fig. 1B).

WY-14,643 escalates ethanol clearance in the *Pex16*$^{fl/fl}$ mice but not in the *Pex16*$^{Alb\text{-}Cre}$ mice

After ethanol feeding, serum levels of ethanol were comparable in the *Pex16*$^{fl/fl}$ mice and *Pex16*$^{Alb\text{-}Cre}$ mice, but WY-14,643 decreased serum ethanol levels in the *Pex16*$^{fl/fl}$ mice but not in the *Pex16*$^{Alb\text{-}Cre}$ mice (Fig. 1D). CYP2E1 was induced by ethanol in both the *Pex16*$^{fl/fl}$ mice and *Pex16*$^{Alb\text{-}Cre}$ mice, but the ethanol induction of CYP2E1 was blunted by WY-14,643 in the *Pex16*$^{fl/fl}$ mice but not in the *Pex16*$^{Alb\text{-}Cre}$ mice (Fig. 1A), implicating that CYP2E1 does not contribute to the lowered serum ethanol levels by WY-14,643. Ethanol induction of CYP2E1 is due to decreased degradation of the ethanol-bound CYP2E1 (2), thus, WY-14,643 suppressed the ethanol induction of CYP2E1 might be due to the

lowered ethanol levels because the basal levels of CYP2E1 without ethanol feeding was not decreased by WY-14,643. ADH1 and ALDH2 expression were not affected by ethanol or WY-14,643 in either the *Pex16*$^{fl/fl}$ mice or *Pex16*$^{Alb\text{-}Cre}$ mice (Fig. 1A), but when liver index is increased, the total contents of ADH1 and ALDH2 will be increased, will ethanol metabolism be increased? After binge ethanol administration by gavage at 2.5 g/kg, blood ethanol clearance was comparable in the *Pex16*$^{fl/fl}$ mice and *Pex16*$^{Alb\text{-}Cre}$ mice (Supplemental-Fig. 2), suggesting that liver size does not affect liver ethanol metabolism. WY-14,643 feeding induced hepatomegaly in the *Pex16*$^{fl/fl}$ mice to the same extent as in the *Pex16*$^{Alb\text{-}Cre}$ mice (Fig. 1C), but WY-14,643 decreased serum levels of ethanol in the *Pex16*$^{fl/fl}$ mice but not in the *Pex16*$^{Alb\text{-}Cre}$ mice (Fig. 1D). Consistently, after a single dose of ethanol gavage at 2.5 g/kg, ethanol clearance was escalated by a 2 weeks of prior WY-14,643 feeding in the *Pex16*$^{fl/fl}$ mice (Fig. 1E) but not in the *Pex16*$^{Alb\text{-}Cre}$ mice (Fig. 1F). These results suggest that WY-14,643-enhanced ethanol metabolism in the *Pex16*$^{fl/fl}$ mice is not due to the enlarged liver mass, either.

Catalase is the enzyme responsible for the WY-14,643-enhanced ethanol metabolism. Indeed, after a single dose of ethanol gavage at 2.5 g/kg, the WY-14,643-enhanced ethanol clearance was observed in *Cat*$^{+/+}$ mice (Fig. 2A) but not observed in *Cat*$^{-/-}$ mice (Fig. 2B). Catalase metabolism of ethanol needs H_2O_2. However, when H_2O_2 concentration is higher, catalase will have a priority to decomposing H_2O_2. Only low concentration of H_2O_2 gradually and continuously released from H_2O_2-generating systems will be used for the ethanol oxidation (7,32). Peroxisomes contain many oxidases such as D-amino acid oxidase, uric acid oxidase, and ACOX. Thus, peroxisomes are good source of H_2O_2 for catalase metabolism of ethanol. ACOX is important considering the Lieber-DeCarli liquid diets containing high content of fat. ACOX continuously oxidizes FFA-derived acyl-CoA to release H_2O_2 for catalase ethanol oxidation. However, unlike ACOX1 that was induced dramatically, catalase was induced moderately (Fig. 1A,1B). Normally, only about 40% of catalase bind with H_2O_2 to form the catalase-H_2O_2 complex, when H_2O_2 is increased, the turnover number of the overall H_2O_2 decomposition reaction will be increased (8). It is possible that when ethanol replaces the second H_2O_2, the turnover number of the reaction of ethanol with the catalase-H_2O_2 complex will still be increased and ethanol metabolism will be enhanced. This might be the reason why moderately induced catalase still dramatically enhanced ethanol metabolism and escalated blood ethanol clearance.

When catalase is not induced yet but ACOX1 is already increased, will catalase metabolism of ethanol still be increased? Time course study showed that after WY-14,643 feeding, PEX16 was induced dramatically after 4 days, PMP70 and catalase were induced after 2 days (Fig 2C), and liver index was also increased after 2 days (Fig. 2D). Interestingly, after only 1 day of WY-14,643 feeding ACOX1 was already induced but catalase was not induced yet (Fig 2C), and live sizes were not increased, either (Fig. 2D). After 1 day of WY-14,643 feeding, 2.5 g/kg ethanol was treated by gavage. Within 2 hours, serum ethanol clearance was not enhanced by WY-14,643, but after 4 hours, serum levels of ethanol were slightly but significantly lowered by the 1-day WY-14,643 feeding (Fig. 2E), suggesting that when catalase is not increased and liver sizes were not increased, ACOX1 induction can also enhance ethanol metabolism, albeit to a small extent. Furthermore, in an acute-on-chronic model, that mice were fed the Lieber-DeCarli ethanol diet containing 0–20 mg/L WY-14,643

for 2 weeks followed by a gavage of 5 g/kg ethanol, decreased serum ethanol by WY-14,643 was partially reversed by ACOX1 inhibitor TrA (Fig. 2F), indicating a pivotal role of ACOX1 in the enhanced ethanol metabolism.

However, ethanol metabolism was not enhanced in the *Pex16*$^{Alb\text{-}Cre}$ mice even though both ACOX1 and catalase were upregulated. Normally, ACOX1 and catalase are mainly located in peroxisomes. In peroxisome matrix, ACOX1 is physically close to catalase so that ACOX1-generated H_2O_2 is readily coupled with catalase for ethanol oxidation. The *Pex16*$^{Alb\text{-}Cre}$ mice lack structural peroxisomes, so the upregulated ACOX1 and catalase were not closely located in the peroxisomal compartment, instead they were extensively distributed in cytosol as shown in Fig. 1B, Supplemental-Fig. 1C and 1D. Thus, intact functional peroxisomes provide an intracellular environment for coupling ACOX1 with catalase to oxidize ethanol. Similarly, catalase also metabolizes methanol in the presence of H_2O_2, and liver fractions containing peroxisomes metabolize much more methanol than liver cytosols (33).

The PPARα-mediated peroxisome proliferation parallels with hepatomegaly (16). After 1 day of WY-14,643 feeding, peroxisome marker PMP70 was not induced yet (Fig. 2C), liver index was not increased, either (Fig. 2D), indicating that peroxisomes were not proliferated yet, suggesting that peroxisome proliferation is induced by chronic treatment of WY-14,643 but not by acute treatment of WY-14,643. Acute treatment of WY-14,643 escalated ethanol clearance (Fig. 2E) to a less extent than chronic treatment of WY-14,643 (Fig. 1E, 2A). Furthermore, WY-14,643-enhanced ethanol clearance was not observed in the *Pex16*$^{Alb\text{-}Cre}$ mice. Therefore, ethanol metabolism is enhanced under peroxisome proliferation.

WY-14,643 ameliorates alcoholic steatosis but enhances alcoholic steatohepatitis in the *Pex16*$^{fl/fl}$ mice but not in the *Pex16*$^{Alb\text{-}Cre}$ mice.

Alcoholic steatosis is a readout of abnormal lipid metabolism. Impaired fatty acid β-oxidation is one of the causes of alcoholic steatosis. WY-14,643 ameliorated alcoholic steatosis and this alleviation was reversed by ACOX1 inhibitor TrA, suggesting an important role of peroxisomal fatty acid β-oxidation in suppressing alcoholic steatosis (15). In the *Pex16*$^{fl/fl}$ mice, alcoholic steatosis as indicated by lipid droplets was observed in the ethanol group but not in the group of ethanol plus WY-14,643 as shown in Fig. 3A H&E staining (its quantification in Supplemental Fig. 3A). Consistently, ethanol induced liver TG accumulation in the *Pex16*$^{fl/fl}$ mice was decreased by WY-14,643 (Fig. 3B). Compared with ethanol alone, ethanol/WY-14,643 suppressed serum TG (Fig. 3C) and tended to reduce serum FFA (Fig. 3D) but tended to increase serum ketone body (Fig. 3E), indicating that lipid metabolism was improved by WY-14,643. Lipid droplets, elevated liver TG, altered serum lipids were not observed in the *Pex16*$^{Alb\text{-}Cre}$ mice. These results suggest that WY-14,643 ameliorates alcoholic steatosis in the *Pex16*$^{fl/fl}$ mice but not in the *Pex16*$^{Alb\text{-}Cre}$ mice.

However, acidophilic degeneration was observed in the mice fed WY-14,643 alone or in combination with ethanol, which was observed in the *Pex16*$^{fl/fl}$ mice but not in the *Pex16*$^{Alb\text{-}Cre}$ mice as shown in Fig. 3A H&E staining (its quantification in Supplemental Fig. 3B). Usually, several initially unrelated lesions contribute to the development of

necrosis (34). WY-14,643 alone did not significantly increase serum levels of ALT yet, but WY-14,643 in combination with ethanol induced serum ALT, indicating an acidophilic necrosis in liver, which was also observed in the *Pex16*$^{fl/fl}$ mice but not in the *Pex16*$^{Alb\text{-}Cre}$ mice (Fig. 3F). Peroxisomes are responsible for about 20% oxygen consumption in liver (35). In response to WY-14,643, ACOX1 was induced to a much greater extent than catalase (Fig. 1B). The disproportionate induction of H_2O_2-generating ACOX and H_2O_2-scavenging catalase was proposed to be responsible for peroxisome-derived oxidative stress (36). Therefore, WY-14,643 induction of ACOX1 has dual effects on liver. On the one hand, the induced ACOX1 increases peroxisomal fatty acid β-oxidation to ameliorate alcoholic steatosis. On the other hand, the induced ACOX1 may promote oxidative liver injury. Usually, ALD advances from steatosis to steatohepatitis, but under peroxisome proliferation, spectrum of ALD is altered. i.e., steatohepatitis was developed with suppressed steatosis.

In the *Pex16*$^{Alb\text{-}Cre}$ mice, ACOX1 and catalase are upregulated to the same levels as WY-14,643-induced ACOX1 and catalase in the *Pex16*$^{fl/fl}$ mice. However, the *Pex16*$^{Alb\text{-}Cre}$ mice did not show evident alcoholic steatosis and WY-14,643-induced acidophilic degeneration. Thus, it is peroxisome proliferation that contributes to the altered spectrum of ALD.

WY-14,643 exerts effects through PPARα but not through Nrf2.

The *ppara*$^{-/-}$ mice develop more severe steatosis in response to ethanol feeding (15, 37). Oxidative stress is an essential factor for the transition of steatosis to steatohepatitis (38). Nrf2 is a redox transcription factor that regulates antioxidant responses and *Nrf2*$^{-/-}$ mice also developed more severe ALD (39). Interestingly, PPARα is upregulated in the *Nrf2*$^{-/-}$ mice (40), implying a compensation of PPARα upon the loss of Nrf2. Previously, we found that WY-14,643-enhanced ethanol metabolism and WY-14,643-suppressed alcoholic steatosis were not observed in the *ppara*$^{-/-}$ mice (13, 15), suggesting that WY-14,643 exerts effects through PPARα. Does Nrf2 also regulate the WY-14,643 effects? In this study, we found that those WY-14,643 effects observed in the WT mice were also observed in the *Nrf2*$^{-/-}$ mice, but when the *Nrf2*$^{-/-}$ mice were abrogated PPARα, these effects were not observable. Therefore, we conclude that WY-14,643 exerts all observed effects through PPARα but not through Nrf2.

As shown in Fig. 4A, PEX16, PMP70, ACOX1, catalase, and CYP4A11 were all induced by WY-14,643 in the *Nrf2*$^{-/-}$ mice as well as in the WT mice but not in the *Nrf2*$^{-/-}$ mice lacking PPARα, i.e., *Ppara*$^{-/-}$/*Nrf2*$^{-/-}$ mice. Liver index was increased by WY-14,643 in the *Nrf2*$^{-/-}$ mice and the WT mice but not in the *Ppara*$^{-/-}$/*Nrf2*$^{-/-}$ mice (Fig. 4B); serum ethanol levels were also decreased by WY-14,643 in the *Nrf2*$^{-/-}$ mice and the WT mice but not in the *Ppara*$^{-/-}$/*Nrf2*$^{-/-}$ mice (Fig. 4C). Ethanol-induced liver TG accumulation was higher in the *Nrf2*$^{-/-}$ mice than in the WT mice, but WY-14,643 blunted the TG accumulation in both the WT mice and the *Nrf2*$^{-/-}$ mice (Fig. 4D). Consistently, H&E staining showed that alcoholic steatosis was more severe in the *Nrf2*$^{-/-}$ mice than in the WT mice, and WY-14,643 attenuated the alcoholic steatosis in both the WT mice and *Nrf2*$^{-/-}$ mice (Fig. 4E). However, in the *Ppara*$^{-/-}$/*Nrf2*$^{-/-}$ mice, ethanol-induced liver TG accumulation was further increased, but WY-14,643 did not suppress the TG accumulation

(Fig. 4D). H&E staining showed that the alcoholic steatosis was extremely severe in the *Ppara*$^{-/-}$/*Nrf2*$^{-/-}$ mice and WY-14,643 failed to ameliorate the severe alcoholic steatosis (Fig. 4E).

In conclusion, WY-14,643 induces PEX16 contributing to peroxisome proliferation. PPARα regulates both peroxisomal fatty acid β-oxidation and peroxisomal ethanol metabolism. Peroxisomal fatty acid β-oxidation initiated by ACOX1 couples with catalase to promote peroxisomal ethanol metabolism. WY-14,643 enhances ethanol metabolism via a PPARα-PEX16-ACOX-catalase network. Absence of PEX16 leads to absence of peroxisomes and upregulation of ACOX1 and catalase. The upregulation of ACOX1 and catalase are mainly located in cytosol and fails to enhance ethanol metabolism. The induced peroxisome proliferation is essential for the enhanced catalase metabolism of ethanol. Nrf2 has no effect on WY-14,643-induced effects.

Supplementary Material

Refer to Web version on PubMed Central for supplementary material.

Acknowledgement

We thank Dr. Jerome Lasker for anti-CYP2E1 IgG.

Financial support statement:

This work was supported in part by NIH grant R01AA024723 to YL and NIH grant P20 GM103434 to the West Virginia IDeA Network of Biomedical Research Excellence.

REFERENCES

1. Lieber CS. (2005). Metabolism of alcohol. Clin Liver Dis. 9, 1–35. [PubMed: 15763227]
2. Lu Y, Cederbaum AI. (2008). CYP2E1 and oxidative liver injury by alcohol. Free Radic Biol Med. 44, 723–738. [PubMed: 18078827]
3. Lu Y, Zhuge J, Wang X, Bai J, Cederbaum AI. Cytochrome P450 2E1 contributes to ethanol-induced fatty liver in mice. Hepatology. 2008 May;47(5):1483–94 [PubMed: 18393316]
4. Lu Y, Cederbaum AI. Cytochrome P450s and Alcoholic Liver Disease. Curr Pharm Des. 2018;24(14):1502–1517. [PubMed: 29637855]
5. Reddy JK, Hashimoto T. Peroxisomal beta-oxidation and peroxisome proliferator-activated receptor alpha: an adaptive metabolic system. Annu Rev Nutr 21: 193–230, 2001. [PubMed: 11375435]
6. Chance B, Sies H, Boveris A. Hydroperoxide metabolism in mammalian organs. Physiol Rev. 1979 Jul;59(3):527–605. [PubMed: 37532]
7. Oshino N, Oshino R, Chance B. The characteristics of the “peroxidatic” reaction of catalase in ethanol oxidation. Biochem J. 1973 Mar;131(3):555–567. [PubMed: 4720713]
8. Oshino N, Jamieson D, Sugano T, Chance B. Optical measurement of the catalase-hydrogen peroxide intermediate (Compound I) in the liver of anaesthetized rats and its implication to hydrogen peroxide production in situ. Biochem J. 1975 Jan;146(1):67–77. [PubMed: 1147905]
9. Handler JA, Thurman RG. Redox interactions between catalase and alcohol dehydrogenase pathways of ethanol metabolism in the perfused rat liver. J Biol Chem. 1990 Jan 25;265(3):1510–1515. [PubMed: 2295642]
10. Handler JA, Thurman RG. Fatty acid-dependent ethanol metabolism. Biochem Biophys Res Commun. 1985 Nov 27;133(1):44–51. [PubMed: 2934065]

11. Handler JA, Thurman RG. Catalase-dependent ethanol oxidation in perfused rat liver. Requirement for fatty-acid-stimulated H2O2 production by peroxisomes. Eur J Biochem. 1988 Sep 15;176(2):477–84. [PubMed: 3416882]
12. Yue R, Chen GY, Xie G, Hao L, Guo W, Sun X, Jia W, Zhang Q, Zhou Z, Zhong W. Activation of PPARα-catalase pathway reverses alcoholic liver injury via upregulating NAD synthesis and accelerating alcohol clearance. Free Radic Biol Med. 2021 Oct;174:249–263. [PubMed: 34390780]
13. Chen X, Xu Y, Denning KL, Grigore A, Lu Y. PPARα agonist WY-14,643 enhances ethanol metabolism in mice: Role of catalase. Free Radic Biol Med. 2021 Jun;169:283–293. [PubMed: 33892114]
14. Xu Y, Denning KL, Lu Y. PPARα agonist WY-14,643 induces adipose atrophy and fails to blunt chronic ethanol-induced hepatic fat accumulation in mice lacking adipose FGFR1. Biochem Pharmacol. 2021 Oct;192:114678. [PubMed: 34265279]
15. Xu Y, Denning KL, Lu Y. PPARα agonist WY-14,643 induces the PLA2/COX-2/ACOX1 pathway to enhance peroxisomal lipid metabolism and ameliorate alcoholic fatty liver in mice. Biochem Biophys Res Commun. 2022 Jul 12;613:47–52. [PubMed: 35526488]
16. Reddy JK. Peroxisome proliferators and peroxisome proliferator-activated receptor alpha: biotic and xenobiotic sensing. Am J Pathol. 2004 Jun;164(6):2305–21. [PubMed: 15161663]
17. Pawlak M, Lefebvre P, Staels B. Molecular mechanism of PPARα action and its impact on lipid metabolism, inflammation and fibrosis in non-alcoholic fatty liver disease. J Hepatol 2015; 62:720–733. [PubMed: 25450203]
18. Fischer M, You M, Matsumoto M, Crabb DW. Peroxisome proliferator-activated receptor alpha (PPARalpha) agonist treatment reverses PPARalpha dysfunction and abnormalities in hepatic lipid metabolism in ethanol-fed mice. J Biol Chem. 2003 Jul 25;278(30):27997–8004. [PubMed: 12791698]
19. Kim PK, Mullen RT, Schumann U, Lippincott-Schwartz J. The origin and maintenance of mammalian peroxisomes involves a de novo PEX16-dependent pathway from the ER. J Cell Biol. 2006 May 22;173(4):521–32. [PubMed: 16717127]
20. Lodhi IJ, Semenkovich CF. Peroxisomes: a nexus for lipid metabolism and cellular signaling. Cell Metab. 2014 Mar 4;19(3):380–92. [PubMed: 24508507]
21. Honsho M, Tamura S, Shimozawa N, Suzuki Y, Kondo N, Fujiki Y. Mutation in PEX16 is causal in the peroxisome-deficient Zellweger syndrome of complementation group D. Am J Hum Genet. 1998 Dec;63(6):1622–30. [PubMed: 9837814]
22. Lee SS, Pineau T, Drago J, Lee EJ, Owens JW, Kroetz DL, Fernandez-Salguero PM, Westphal H, Gonzalez FJ. Targeted disruption of the alpha isoform of the peroxisome proliferator-activated receptor gene in mice results in abolishment of the pleiotropic effects of peroxisome proliferators. Mol Cell Biol. 1995;15(6):3012–22. [PubMed: 7539101]
23. Chan K, Lu R, Chang JC, Kan YW. NRF2, a member of the NFE2 family of transcription factors, is not essential for murine erythropoiesis, growth, and development. Proc Natl Acad Sci U S A. 1996 Nov 26;93(24):13943–8. [PubMed: 8943040]
24. Ho YS, Xiong Y, Ma W, Spector A, Ho DS. Mice Lacking Catalase Develop Normally but Show Differential Sensitivity to Oxidant Tissue Injury. J Biol Chem. 2004 Jul 30;279(31):32804–12. [PubMed: 15178682]
25. Eagon PK. Alcoholic liver injury: influence of gender and hormones. World J Gastroenterol. 2010 Mar 21;16(11):1377–84. [PubMed: 20238405]
26. Bertola A, Mathews S, Ki SH, Wang H, Gao B. Mouse model of chronic and binge ethanol feeding (the NIAAA model). Nat Protoc. 2013 Mar;8(3):627–37. [PubMed: 23449255]
27. Zeng J, Deng S, Wang Y, Li P, Tang L, Pang Y. Specific Inhibition of Acyl-CoA Oxidase-1 by an Acetylenic Acid Improves Hepatic Lipid and Reactive Oxygen Species (ROS) Metabolism in Rats Fed a High Fat Diet. J Biol Chem. 2017 Mar 3;292(9):3800–3809. [PubMed: 28077576]
28. Baes M, Van Veldhoven PP. Hepatic dysfunction in peroxisomal disorders. Biochim Biophys Acta. 2016 May;1863(5):956–70. [PubMed: 26453805]

29. Singh I, Kremser K, Ghosh B, Singh AK, Pai S. Abnormality in translational regulation of catalase expression in disorders of peroxisomal biogenesis. J Neurochem. 1996 Dec;67(6):2373–8. [PubMed: 8931469]

30. Kim PK, Mullen RT. PEX16: a multifaceted regulator of peroxisome biogenesis. Front Physiol. 2013 Sep 3;4:241 [PubMed: 24027535]

31. LeeRackles E, Witting M, Forné I, Zhang X, Zacherl J, Schrott S, Fischer C, Ewbank JJ, Osman C, Imhof A, Rolland SG. Reduced peroxisomal import triggers peroxisomal retrograde signaling. Cell Rep. 2021 Jan 19;34(3):108653. [PubMed: 33472070]

32. Keilin David and Hartree EF. Coupled oxidation of alcohol. Proceedings of the Royal Society B, 1936, 119 (813): 141–159

33. Makar AB, Mannering GJ. Role of the intracellular distribution of hepatic catalase in the peroxidative oxidation of methanol. Mol Pharmacol. 1968 Sep;4(5):484–91. [PubMed: 4972129]

34. Decker K. Mechanisms and mediators in hepatic necrosis. Gastroenterol Jpn. 1993 Mar;28 Suppl 4:20–25.

35. De Duve C, Baudhuin P. Peroxisomes (microbodies and related particles). Physiol Rev. 1966 Apr;46(2):323–57. [PubMed: 5325972]

36. Schrader M, Fahimi HD. Peroxisomes and oxidative stress. Biochim Biophys Acta. 2006 Dec;1763(12):1755–66. [PubMed: 17034877]

37. Nakajima T, Kamijo Y, Tanaka N, Sugiyama E, Tanaka E, Kiyosawa K, Fukushima Y, Peters JM, Gonzalez FJ, Aoyama T. Peroxisome proliferator-activated receptor alpha protects against alcohol-induced liver damage. Hepatology. 2004 Oct; 40(4):972–80. [PubMed: 15382117]

38. Font-Burgada J, Sun B, Karin M. Obesity and cancer: the oil that feeds the flame. Cell Metab 23: 48–62, 2016. [PubMed: 26771116]

39. Lamlé J, Marhenke S, Borlak J, von Wasielewski R, Eriksson CJ, Geffers R, Manns MP, Yamamoto M, Vogel A. Nuclear factor-eythroid 2-related factor 2 prevents alcohol-induced fulminant liver injury. Gastroenterology. 2008 Apr;134(4):1159–68. [PubMed: 18395094]

40. Chen X, Ward SC, Cederbaum AI, Xiong H, Lu Y. Alcoholic fatty liver is enhanced in CYP2A5 knockout mice: The role of the PPARα-FGF21 axis. Toxicology. 2017 Mar 15;379:12–21. [PubMed: 28131861]

Highlights:

- Peroxisomes provide an intracellular environment for ACOX1 coupling with catalase to promote ethanol metabolism.
- WY-14,643 induces PEX16 contributing to peroxisome proliferation, and absence of PEX16 leads to absence of peroxisomes and upregulation of ACOX1 and catalase.
- Due to lacking peroxisomes, the upregulation of ACOX1 and catalase are located in cytoplasm and fails to enhance ethanol metabolism.
- WY-14,643 exerts all effects via PPARα but not via Nrf2.

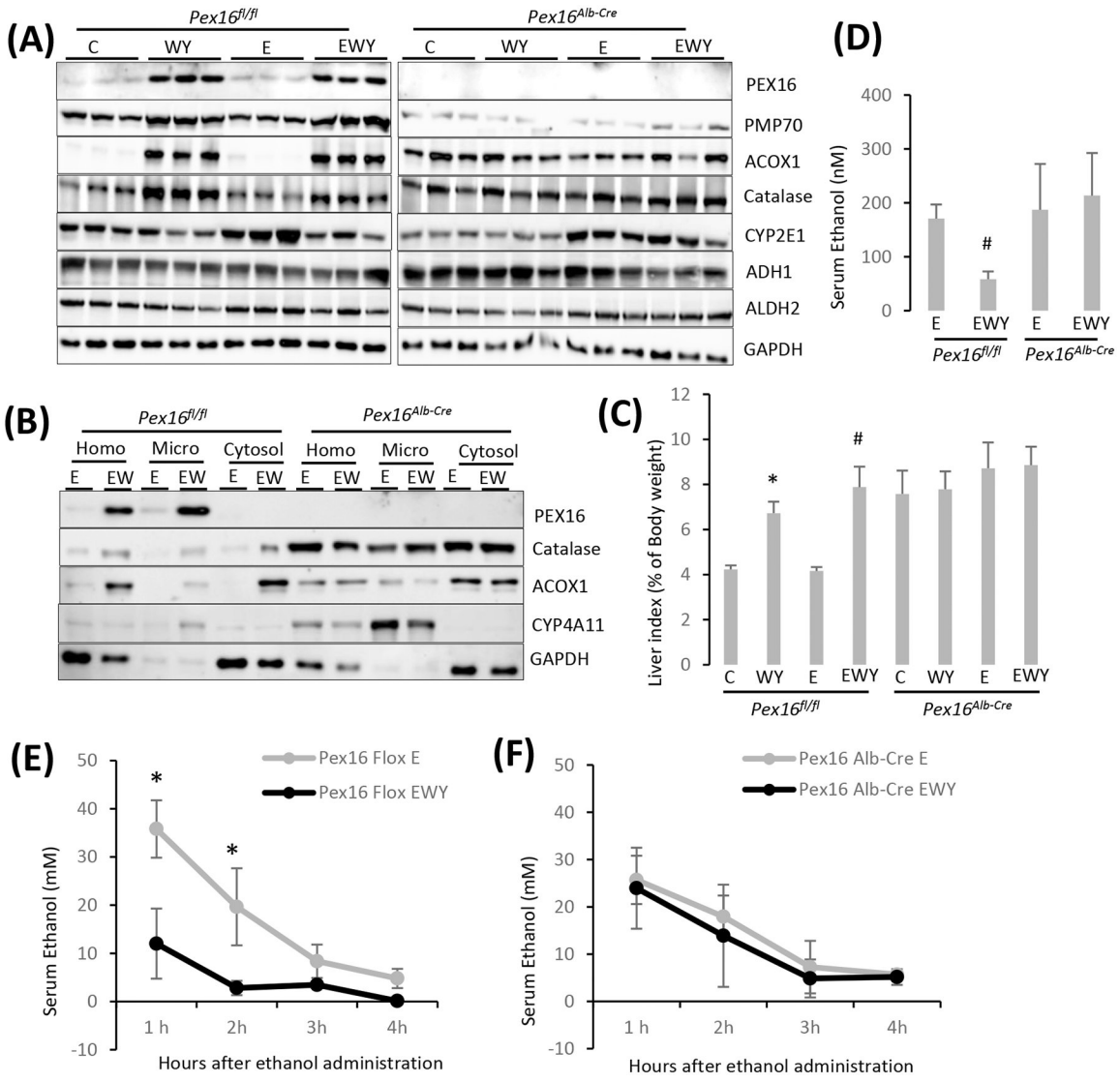

Figure 1.

WY-14,643 induces ACOX1 and catalase and enhances ethanol metabolism in the *Pex16*$^{fl/fl}$ mice but not in the *Pex16*$^{Alb\text{-}Cre}$ mice.

(A-D) The female mice were fed Lieber-DeCarli liquid control and ethanol diet containing 0–10 mg/L of WY-14,643 for 25 days. (A) Effects of WY-14,643 on hepatic expression of peroxisomal enzymes and major ethanol metabolism enzymes in the *Pex16*$^{fl/fl}$ mice and *Pex16*$^{Alb\text{-}Cre}$ mice. (B) Microsomal and cytosolic distribution of WY-14,643-induced PEX16, catalase, ACOX1, and CYP4A11. (C) Liver index indicating that WY-14,643 induced hepatomegaly in the *Pex16*$^{fl/fl}$ mice but not in the *Pex16*$^{Alb\text{-}Cre}$ mice (n=3–4). (D) Effects of WY-14,643 on serum ethanol levels (n=3–4). * P<0.05, compared with C group; # P<0.05, compared with E group. C, control; WY, WY-14,643; E, ethanol; EWY, ethanol+WY-14,643.

(E-F) The male mice were fed Lieber-DeCarli liquid control diet containing 20 mg/L of WY-14,643 for 2 weeks followed by a single dose of ethanol gavage at 2.5 g/kg. The blood was collected after 1, 2, 3, and 4 hours. WY-14,643 escalated blood ethanol clearance in the

PEX16$^{fl/fl}$ mice (E) but not in the *PEX16*$^{Alb\text{-}Cre}$ mice (F). * P<0.05, compared with E groups (n=3). E, binge ethanol; EWY, binge ethanol+WY-14,643.

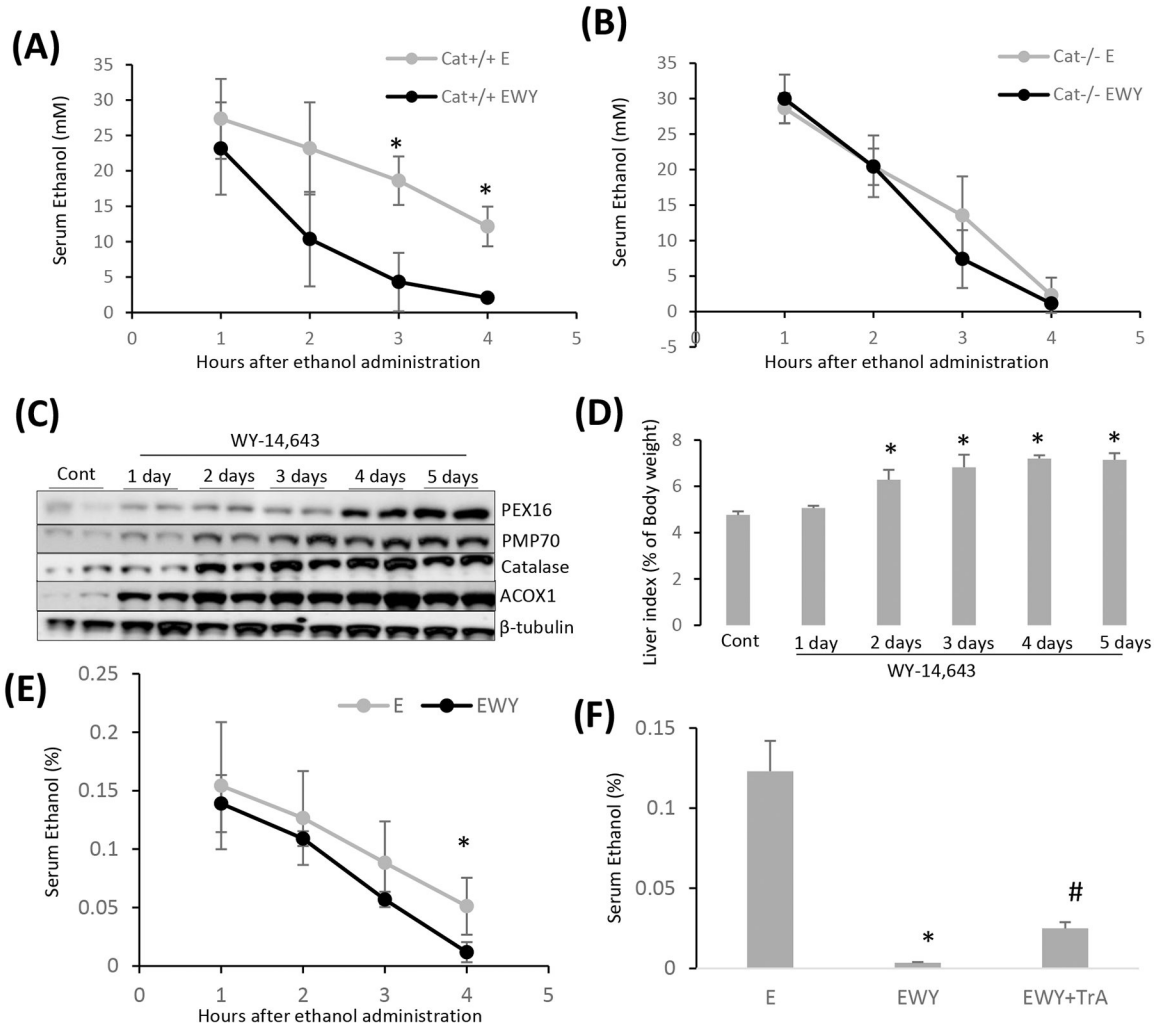

Figure 2.

Catalase and ACOX1 contribute to escalated ethanol clearance by WY-14,643.

(A-B) The male mice were fed Lieber-DeCarli liquid control diet containing 0–20 mg/L of WY-14,643 for 2 weeks followed by a single dose of ethanol gavage at 2.5 g/kg. The blood was collected after 1, 2, 3, and 4 hours. The escalated ethanol clearance by WY-14,643 was observed in the $Cat^{+/+}$ mice (A) but not in the $Cat^{-/-}$ mice (B). * P<0.05, compared with $Cat^{-/-}$ mice (n=3).

(C-D) The male mice were fed Lieber-DeCarli liquid control diet containing 0–20 mg/L of WY-14,643 for 1–5 days. PEX16, PMP70, catalase and ACOX1 were induced in different patterns (C) and liver index was increased after 2 days. * P<0.05, compared with Control group (n=3).

(E) The male mice were fed Lieber-DeCarli liquid control diet containing 0–20 mg/L of WY-14,643 for 1 day followed by a single dose of ethanol gavage at 2.5 g/kg. The blood was collected after 1, 2, 3, and 4 hours. * P<0.05, compared with WY-14,643 group (n=3).

(F) Decreased serum ethanol by WY-14,643 was reversed by ACOX1 inhibitor TrA. The male mice were fed Lieber-DeCarli liquid ethanol diet containing 0–20 mg/L of WY-14,643 for 2 weeks followed by a single dose of 5 g/kg ethanol gavage. TrA was injected (10

mg/kg) twice at 30 min and 24 h before ethanol gavage. * $P<0.05$, compared with E group (n=3); # $P<0.05$, compared with EWY group.

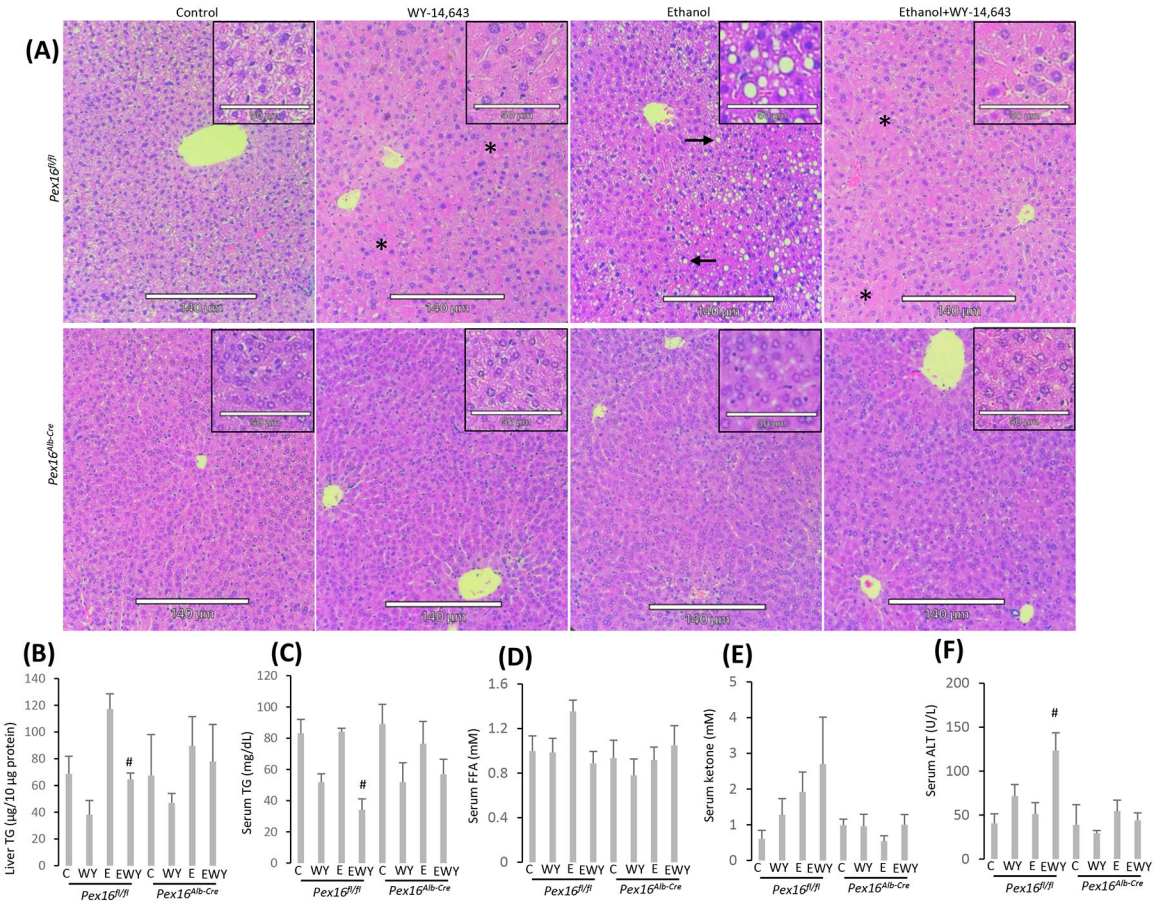

Figure 3.

Ethanol feeding induced fatty liver in the *Pex16*$^{fl/fl}$ mice but not in the *Pex16*$^{Alb\text{-}Cre}$ mice. The female mice were fed Lieber-DeCarli liquid control and ethanol diet containing 0–10 mg/L of WY-14,643 for 25 days. (A) H&E staining in liver sections indicating that ethanol induced fatty liver in the *Pex16*$^{fl/fl}$ mice but not in the *Pex16*$^{Alb\text{-}Cre}$ mice and WY-14,643 blunted the alcoholic fatty liver in the *Pex16*$^{fl/fl}$ mice. Arrows show lipid droplets. Stars show acidophilic degeneration. Scale bars = 140 μm. (B) WY-14,643 significantly decreased ethanol-induced hepatic TG accumulation in the *Pex16*$^{fl/fl}$ mice (n=3–4) but not in the *Pex16*$^{Alb\text{-}Cre}$ mice (n=4). (C) WY-14,643 decreased serum TG in the *Pex16*$^{fl/fl}$ mice (n=3–4) but not in the *Pex16*$^{Alb\text{-}Cre}$ mice (n=4). (D) Serum FFA was not significantly changed by WY-14,643 (n=3–4). (E) WY-14,643 tended to increase serum ketone in the *Pex16*$^{fl/fl}$ mice (n=3–4) but not in the *Pex16*$^{Alb\text{-}Cre}$ mice (n=4). (F) WY-14,643 in combination with ethanol increased serum ALT in the *Pex16*$^{fl/fl}$ mice (n=3–4) but not in the *Pex16*$^{Alb\text{-}Cre}$ mice (n=4). * P<0.05, compared with C group; # P<0.05, compared with E group. C, control; WY, WY-14,643; E, ethanol; EWY, ethanol+WY-14,643.

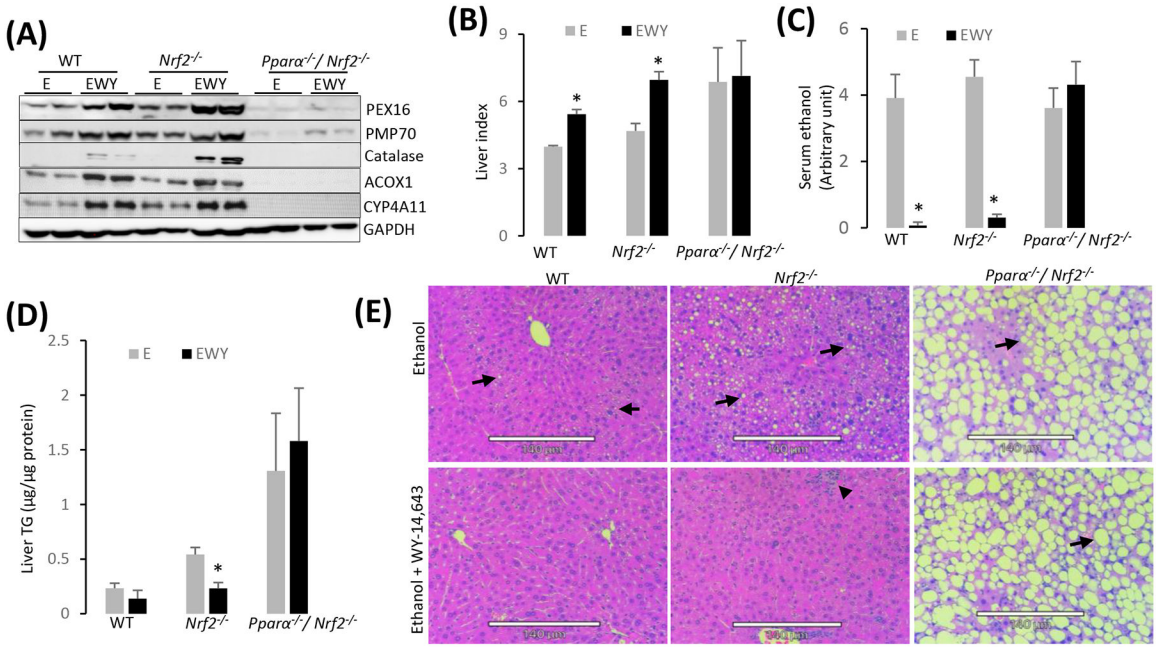

Figure 4.

The effects of WY-14,643 are regulated by PPARα but not by Nrf2. The female WT mice, *Nrf2*$^{-/-}$ mice, and *Pparα*$^{-/-}$/*Nrf2*$^{-/-}$ mice were fed Lieber-DeCarli liquid ethanol diet containing 10 mg/L of WY-14,643 for 18 days. (A) WY-14,643-induced hepatic proteins. (B) Liver index (n=3–4). (C) Serum ethanol levels (n=3–4). (D) Liver TG contents (n=3–4). (E) H&E staining. Arrows show lipid droplets. Arrowhead shows inflammatory foci. Scale bars =140μm.

* P<0.05, compared with E group. E, ethanol; EWY, ethanol+WY-14,643.